Measurement of the Inclusive Jet Cross Section using the K_T algorithm in $p\overline{p}$ Collisions at $\sqrt{s} = 1.96$ TeV

The CDF Collaboration

Draft version 0.2

We report on the measurement of the inclusive jet cross section in $p\overline{p}$ collisions at $\sqrt{s} = 1.96$ TeV. Jets are searched for using the longitudinally invariant K_T algorithm. The measurement is carried out for jets with rapidity $0.1 < |Y^{jet}| < 0.7$ and transverse momentum in the range $54 < P_T^{jet} < 700$ GeV/c, and is corrected to the hadron level. The measured cross section is in good agreement with NLO perturbative QCD predictions.

To be read together with the CDF note 7576

The measurement of the inclusive jet cross section as a function of the jet transverse momentum, P_T^{jet}, in $p\overline{p}$ collisions at $\sqrt{s} = 1.96$ TeV constitutes a stringent test of perturbative QCD (pQCD) [1] predictions over more than eight orders of magnitude and is sensitive to the presence of new physics beyond the standard model. The pQCD calculations are written as matrix elements, describing the hard interaction between partons, convoluted with parton density functions (PDFs) [2,3] in the proton and antiproton that require input from the experiments. In particular, inclusive jet production measurements from Run I [4] have been used to partially constrain the gluon distribution in the proton at high x-Bjorken. The increased center-of-mass energy and integrated luminosity in Run II at the Tevatron have allowed to extend the measured jet cross section to jets with transverse momentum up to about 700 GeV/c. This letter presents a measurement of the inclusive jet production cross section as a function of P_T^{jet} for jets with $P_T^{jet} > 54$ GeV/c and rapidity [5] in the region $0.1 < |Y^{jet}| < 0.7$, where jets are searched for using the longitudinally invariant K_T algorithm [6,7] in the laboratory frame. The measurements are corrected to the hadron level [8] and compared to pQCD NLO predictions [9]. Similar measurements have been carried out using cone-based jet algorithms [4,10] for which an additional parameter [7] must be introduced in the pQCD predictions to mimic the splitting and merging prescription of overlapping cones defined in the data.

The hadronic final states in hadron-hadron collisions are characterized by the presence of soft hadronic activity produced by initial-state soft-gluon radiation and the interaction between the proton and antiproton remnants (the so-called *underlying event*), in addition to collimated jets of hadrons along the direction of the scattered partons originated by the hard interaction. A proper comparison between the measured jet cross section at the hadron level and the pQCD prediction at the parton level requires additional corrections to account for the contribution to the measured P_T^{jet} spectrum from the underlying event and hadronization processes that become important at low P_T^{jet}; this could explain the marginal agreement between the data and the pQCD NLO predictions observed in previous jet measurements using the K_T algorithm in Run I [11]. A number of precise measurements have been carried out in Run II [12,13] indicating that a good description of the underlying event and the jet fragmentation into hadrons is achieved by tuning Monte Carlo models.

The CDF II detector is described in detail in [14]. Here, the sub-detectors most relevant for this analysis are briefly discussed. The detector has a charged particle tracking system immersed in a 1.4 T magnetic field, aligned coaxially with the beam line. A silicon microstrip detector [15] provides tracking over the radial range 1.35 to 28 cm and covers the pseudorapidity range $|\eta| \leq 2$. A 3.1 m long open-cell drift chamber, the Central Outer Tracker (COT) [16], covers the radial range from 44 to 132 cm and provides tracking coverage for $|\eta| \leq 1$. Segmented sampling calorimeters, arranged in a projective tower geometry, surround the tracking system and measure the energy flow of interacting particles in $|\eta| \leq 3.6$. The CDF central barrel calorimeter [17] is unchanged from Run I and covers the region $|\eta| < 1$. It consists of an electromagnetic (CEM) calorimeter and an hadronic (CHA) calorimeter segmented into 480 towers of size 0.1 in η and 15° in ϕ. The end-wall hadronic (WHA) calorimeter [18] complements the coverage of the central barrel calorimeter in the region $0.6 < |\eta| < 1.0$ and provides additional forward coverage out to $|\eta| < 1.3$. In Run II, new forward scintillator-plate calorimeters [19] replaced the original Run I gas calorimeter system. The new plug electromagnetic (PEM) calorimeter covers the region $1.1 < |\eta| < 3.6$ while the new hadronic (PHA) calorimeter provides coverage in the $1.3 < |\eta| < 3.6$ region. The calorimetry has a crack at $\eta = 0$ (between the two halves of the central barrel calorimeter) and two cracks at $\eta = \pm 1.1$ (in the region between the WHA and the plug calorimeters). The measured energy resolutions for electrons in the electromagnetic calorimeters are $14\%/\sqrt{E_T}$ (CEM) and $16\%/\sqrt{E} \oplus 1\%$ (PEM) where the units are expressed in GeV. The single-pion energy resolutions in the hadronic calorimeters, as determined in test-beam data, are $75\%/\sqrt{E_T}$ (CHA), $80\%/\sqrt{E}$ (WHA) and $80\%/\sqrt{E} \oplus 5\%$ (PHA). Cherenkov counters located in the $3.7 < |\eta| < 4.7$ region [20] measure the average number of inelastic $p\overline{p}$ collisions per bunch crossing and thereby determine the beam luminosity.

Monte Carlo event samples are used to determine the response of the detector and the correction factors to the hadron level. The generated samples are passed through a full CDF detector simulation (based on GEANT3 [21] where the GFLASH [22] package is used to simulate the energy deposition in the calorimeters), and then reconstructed and analyzed using the same analysis chain as in the data. Samples of simulated inclusive jet events have been generated using the PYTHIA 6.203 [23] and HERWIG 6.4 [24] Monte Carlo generators. CTEQ5L [25] parton distribution functions are used for the proton and antiproton. The PYTHIA samples have been created using a special tuned set of parameters, denoted as PYTHIA-Tune A [26], that includes enhanced contributions from initial-state gluon radiation and secondary parton interactions between remnants. Tune A was determined as a result of dedicated studies of the underlying event using the CDF Run I data [27] and it has been shown to properly describe the measured jet shapes in Run II [12]. In the case of PYTHIA, fragmentation into hadrons is carried out using the string model [28] as implemented in JETSET [29], while HERWIG implements the cluster model [30].

The longitudinally invariant K_T algorithm is used to reconstruct jets from the energy deposits in the calorime-

ter towers with transverse momentum above 0.1 GeV/c. The quantities:

$$\mathrm{K_{T\ (i)}} = \mathrm{P^2_{T,i}}\ ;\ \mathrm{K_{T\ (i,j)}} = \min(\mathrm{P^2_{T,i}}, \mathrm{P^2_{T,j}}) \cdot \frac{\Delta \mathrm{R^2_{i,j}}}{\mathrm{D^2}} \quad (1)$$

are computed for each tower and pair or towers, where $\mathrm{P_{T,i}}$ denotes the transverse momentum of the $\mathrm{i^{th}}$ tower, $\Delta R_{\mathrm{i,j}}$ is the distance ($Y - \phi$ space) between each pair of towers and D is a parameter that approximately controls the size of the jet. All $\mathrm{K_{T\ (i)}}$ and $\mathrm{K_{T\ (i,j)}}$ values are then collected into a single sorted list that is input to the algorithm. In the jet algorithm, if the smallest quantity is of the type $\mathrm{K_{T\ (i)}}$ the corresponding tower is called "*jet*" and removed from the list. Otherwise, if the smallest quantity is of the type $\mathrm{K_{T\ (i,j)}}$, the towers are combined into a cluster by summing up their four-vector components. The procedure above is iterated until the list becomes empty. The jet transverse momentum, rapidity and azimuthal angle, as determined using the calorimeter towers, are denoted as $\mathrm{P^{jet}_{T,CAL}}$, $\mathrm{Y^{jet}_{CAL}}$ and $\phi^{\mathrm{jet}}_{\mathrm{CAL}}$, respectively. The same jet algorithm is applied to the final-state particles in Monte Carlo generated events to search for jets at the hadron level. In this case, no cut on the minimum transverse momentum of the particles is applied. The resulting hadron-level jet variables are denoted as $\mathrm{P^{jet}_{T,HAD}}$, $\mathrm{Y^{jet}_{HAD}}$ and $\phi^{\mathrm{jet}}_{\mathrm{HAD}}$.

The measurements presented in this letter correspond to a total integrated luminosity of 385 ± 22 pb^{-1} of data collected by the CDF experiment in Run II. Online, events are selected using three-level trigger paths [31], based on the measured energy deposits in the calorimeter towers, with several different thresholds on the jet transverse energies [12]. Offline, jets are reconstructed using the $\mathrm{K_T}$ algorithm, as explained above, with $D = 0.7$. For each trigger data sample, the threshold on the minimum $\mathrm{P^{jet}_{T,CAL}}$ is chosen in such a way that the trigger is fully efficient in the whole kinematic region under study. The events are required to have at least one jet with rapidity in the region $0.1 < |\mathrm{Y^{jet}_{CAL}}| < 0.7$ and corrected transverse momentum (see below) above 54 GeV/c. The events are selected to have at least one reconstructed primary vertex with z-position within 60 cm around the nominal interaction point. In order to remove beam-related backgrounds and cosmic rays, particularly dangerous at high $\mathrm{P^{jet}_T}$ (where the QCD cross section is very small), the events are required to fulfill $\not{E}_T/\sqrt{\Sigma E_T} < F(\mathrm{P^{leading\ jet}_{T,CAL}})$, where $\not{E}_T$ denotes the missing transverse energy and ΣE_T is the total transverse energy of the event, as measured using calorimeter towers with transverse energy above 100 MeV. The threshold function $F(\mathrm{P^{leading\ jet}_{T,CAL}})$ is defined as $F(\mathrm{P^{leading\ jet}_{T,CAL}}) = \min(2 + \frac{5}{400} \times \mathrm{P^{leading\ jet}_{T,CAL}}, 7)$, where $\mathrm{P^{leading\ jet}_{T,CAL}}$ is the uncorrected transverse momentum of the leading jet. This cut is designed to have very high background-rejection power while preserves more than 95% of the QCD events, as determined from Monte Carlo. A visual scan over the events in the tail of the $\mathrm{P^{jet}_{T,CAL}}$ distribution, above 400 GeV/c, confirmed that they are all consistent with QCD final states.

The jet transverse momentum measured in the calorimeter includes additional contributions as result of multiple proton-antiproton interactions per bunch crossing at high Tevatron instantaneous luminosity. This mainly affects the measured cross section at low $\mathrm{P^{jet}_T}$, where the contributions become sizable. The data used in this measurement was collected at Tevatron instantaneous luminosities in the range between $0.2 \times 10^{31}\mathrm{cm}^{-2}\mathrm{s}^{-1}$ and $9.6 \times 10^{31}\mathrm{cm}^{-2}\mathrm{s}^{-1}$ with an average of $2.6 \times 10^{31}\mathrm{cm}^{-2}\mathrm{s}^{-1}$, for which less than one interaction per bunch crossing is expected. At the highest instantaneous luminosities considered, an average of two interactions per bunch crossing are produced. In CDF, multiple interactions are identified via the presence of additional primary vertices inside the tracking volume. The measured jet transverse momenta are corrected for the effect of multiple proton-antiproton interactions by removing a certain amount of transverse momentum, $\epsilon_{0.7}$, for each additional primary vertex observed in the event. A factor $\epsilon_{0.7} = 1.62^{+0.70}_{-0.46}$ GeV/c is determined from the data by requiring that, after the correction is applied, the ratio of cross sections at low and high instantaneous luminosities does not show any $\mathrm{P^{jet}_T}$ dependence. The errors quoted on $\epsilon_{0.7}$ reflect a conservative estimation of its uncertainty and is included in the study of the systematic uncertainties on the final measurement.

The reconstruction of the jet variables in the calorimeter is studied using Monte Carlo event samples and matched pair of jets ($Y - \phi$ space) at the calorimeter and hadron levels. These studies indicate that the angular variables of the jet are reconstructed in the calorimeter with no significant systematic shift and a resolution better than 0.05 units in Y and ϕ at low $\mathrm{P^{jet}_{T,CAL}}$, that improves as $\mathrm{P^{jet}_{T,CAL}}$ increases. The jet transverse momentum measured in the calorimeter systematically underestimates that of the hadron level jet, which is mainly attributed to the non-compensating nature of the calorimeter [32]. For jets with $\mathrm{P^{jet}_{T,CAL}}$ about 50 GeV/c, the jet transverse momentum is reconstructed with an average shift of -19% and a resolution of 14%. The jet reconstruction improves as $\mathrm{P^{jet}_{T,CAL}}$ increases. For jets with $\mathrm{P^{jet}_{T,CAL}}$ about 500 GeV/c, the jet transverse momentum is reconstructed with an average shift of -5% and a resolution of 7%. In order to evaluate how well the Monte Carlo reproduces the jet energy resolutions observed in the data, the bisector method [33] is employed. The estimated detector resolutions in data and Monte Carlo agree within a relative uncertainty of $\pm 8\%$ over the whole $\mathrm{P^{jet}_{T,CAL}}$ range.

The measured $\mathrm{P^{jet}_{T,CAL}}$ distribution is corrected back to the hadron level using Monte Carlo. PYTHIA-Tune A

provides a reasonable description of the different quantities and is used to determine the correction factors in the unfolding procedure. In order to avoid any bias on the correction factors due to the particular PDFs used during the generation of the Monte Carlo samples, which translates into slightly different simulated $P^{jet}_{T,CAL}$ distributions, PYTHIA-Tune A is re-weighted until it perfectly follows the measured $P^{jet}_{T,CAL}$ spectrum in the data. The unfolding is carried out in two steps. First, an average correction is extracted from the Monte Carlo using matched pair of jets at the calorimeter and hadron levels. The correlation $< P^{jet}_{T,HAD} - P^{jet}_{T,CAL} >$ vs $< P^{jet}_{T,CAL} >$, calculated in bins of $(P^{jet}_{T,HAD} + P^{jet}_{T,CAL})/2$, is used to extract multiplicative correction factors which are then applied to the measured jets to obtain the corrected transverse momenta, $P^{jet}_{T,COR}$. The uncorrected cross section is defined in bins of $P^{jet}_{T,COR}$ as

$$\frac{d^2\sigma}{dP^{jet}_{T,COR} dY^{jet}_{CAL}} = \frac{1}{L} \frac{N^{jet}_{COR}}{\Delta P^{jet}_{T,COR}\ \Delta Y^{jet}_{CAL}}, \qquad (2)$$

where N^{jet}_{COR} denotes the total number of jets measured in a given $P^{jet}_{T,COR}$ bin, $\Delta P^{jet}_{T,COR}$ is the size of the bin, ΔY^{jet}_{CAL} denotes the region in Y^{jet}_{CAL} considered and L is the total luminosity of the data sample. Second, the measurements are corrected for acceptance and smearing effects back to the hadron level using a bin-by-bin unfolding procedure, which also account for the efficiency of the selection criteria. The unfolding factors,

$$U(P^{jet}_{T,COR}) = \frac{d^2\sigma/dP^{jet}_{T,HAD} dY^{jet}_{HAD}}{d^2\sigma/dP^{jet}_{T,COR} dY^{jet}_{CAL}}, \qquad (3)$$

are extracted from Monte Carlo and applied to the measured $P^{jet}_{T,COR}$ distribution in the data to obtain the final result. The factor $U(P^{jet}_{T,COR})$ increases with $P^{jet}_{T,COR}$ and varies between 1.04 at low $P^{jet}_{T,COR}$ and 1.3 at very high $P^{jet}_{T,COR}$.

A detailed study of the different systematic uncertainties was carried out [34]. The measured jet energies were varied by ±2% (at low P^{jet}_T) and ±3% (at very high P^{jet}_T) [35] to account for the uncertainty on the absolute energy scale in the calorimeter; this introduces an uncertainty on the final measurement which varies between ±10% at low P^{jet}_T and $^{+55\%}_{-40\%}$ at high P^{jet}_T. A ±8% uncertainty on the jet energy resolution introduces an uncertainty in the measured cross section between 2% at low P^{jet}_T and 8% at high P^{jet}_T. The unfolding procedure was repeated using HERWIG instead of PYTHIA-Tune A to account for the uncertainty on the modeling of the parton cascades and the jet fragmentation into hadrons; the maximum effect on the measured cross section is of the order of 5% at low P^{jet}_T. The unfolding procedure was carried out using unweighted PYTHIA-Tune A; the effect on the measured cross section is negligible for jets with $P^{jet}_T \leq 400$ GeV/c and introduces a 4% uncertainty at very high P^{jet}_T. The quoted uncertainty on $\epsilon_{0.7}$ was taken into account; the effect on the measured cross section is less than 3% and negligible for jets with $P^{jet}_T \geq 200$ GeV/c. Finally, other sources of systematic uncertainties, related to the event selection criteria, have been considered and found to contribute less than 1% to the total systematic uncertainty on the measurement. Positive and negative deviations with respect to the nominal values in each P^{jet}_T bin are added separately in quadrature to the statistical errors. An additional 5.8% uncertainty on the total luminosity is not included.

The corrected inclusive jet cross section, $\frac{d^2\sigma}{dP^{jet}_T dY^{jet}}$, refers to K_T jets at the hadron level with $D = 0.7$ in the region $0.1 < |Y^{jet}| < 0.7$ and $P^{jet}_T > 54$ GeV/c. Figure 1 shows the measured cross section as a function of P^{jet}_T compared to NLO pQCD predictions. The measured data points are collected in Table I. The data decreases by more than eight orders of magnitude as P^{jet}_T increases from 54 GeV/c up to P^{jet}_T of the order of 700 GeV/c. The NLO pQCD predictions are computed using the

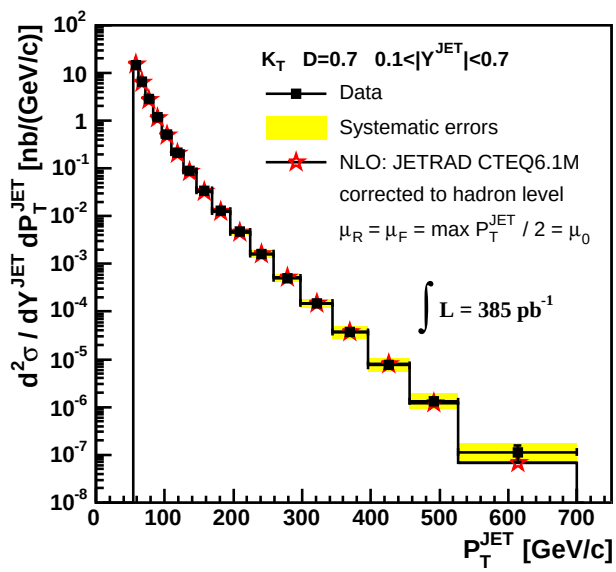

FIG. 1. Measured inclusive jet cross section (black dots) as a function of P^{jet}_T for jets with $P^{jet}_T > 54$ GeV/c and $0.1 < |Y^{jet}| < 0.7$, compared to NLO pQCD predictions (open stars). The shaded band shows the total systematic uncertainty on the measurement.

JETRAD program [9] with CTEQ6.1M PDFs and the renormalization and factorization scales (μ_R and μ_F) set to $\mu_0 = \max(P^{jet}_T)/2$. Different sources of uncertainty in the theoretical predictions were considered. The renormalization and factorization scales were varied from μ_0 to $2\mu_0$ in order to estimate the effect of terms beyond NLO in the calculation; this reduces the theoretical pre-

diction by 2% at low P_T^{jet} and 8% at high P_T^{jet}. The uncertainty due to the PDFs was computed using the Hessian method [36] taking into account $\pm 1\sigma$ variations along each direction in the CTEQ6.1M parameter space; this introduces an uncertainty on the theoretical prediction that increases from $^{+20\%}_{-10\%}$ at low P_T^{jet} to $^{+70\%}_{-30\%}$ at very high P_T^{jet}, and it is dominated by the variation of those parameters associated to the gluon PDF.

The theoretical prediction includes an additional correction factor, $C_{HAD}(P_T^{jet})$, (see Fig. 2 and Table I) that approximately accounts for non-perturbative contributions coming from the underlying event and fragmentation into hadrons, which are not present in the pQCD calculation. As already mentioned, this correction factor is necessary for an adequate comparison between the measured jet cross section at the hadron level and the fixed-order parton-level pQCD prediction. The correction factor $C_{HAD}(P_T^{jet})$ was estimated, using PYTHIA-Tune A, as the difference between the nominal $P_{T,HAD}^{jet}$ distribution and the one obtained after turning off the interactions between proton and antiproton remnants and the JETSET string fragmentation in the Monte Carlo. The parton-to-hadron correction shows a strong P_T^{jet} dependence and increases as P_T^{jet} decreases. For jets with P_T^{jet} about 54 GeV/c the correction is about 1.2. The uncertainty on $C_{HAD}(P_T^{jet})$ is of the order of 13% at low P_T^{jet}, as determined from the difference between the parton-to-hadron correction factors obtained using HERWIG instead of PYTHIA-Tune A.

Figure 3 shows the ratio data/theory as a function of P_T^{jet}. Good agreement is observed between the measured cross section and the pQCD NLO predictions over the whole P_T^{jet} range under study. In particular, no significant deviation from the QCD prediction is observed at high P_T^{jet}. The total uncertainty on the measurement is dominated by the uncertainty on the absolute jet energy scale, while the precision of the theoretical calculation is mainly limited by the present knowledge of the gluon PDF in the proton at high x-Bjorken. In addition, Fig. 3 shows the ratio between pQCD predictions with different μ_R and μ_F scales, as discussed above, and different PDFs set, where MRST2004 is used instead of CTEQ6.1M. The latter changes the pQCD prediction by +10% at low P_T^{jet} and −15% at high P_T^{jet}, well inside the theoretical and experimental uncertainties.

Finally, the complete analysis was repeated using different values for the D parameter in the K_T algorithm ($D = 0.5$ and $D = 1.0$) [34]. In both cases, good agreement was again observed between the measured cross sections and the NLO pQCD predictions in the whole range in P_T^{jet}. This validates the experimental procedure followed to determine the cross section and demonstrates a good control of the parton-to-hadron correction factors applied to the pQCD predictions. As the D parameter decreases (increases) the measurement becomes less (more) sensitive to the presence and proper modeling of the non-perturbative underlying event contributions. For $D = 0.5$ ($D = 1.0$) a parton-to-hadron correction factor $C_{HAD} = 1.1$ ($C_{HAD} = 1.4$) must be applied to the theoretical predictions at low P_T^{jet}.

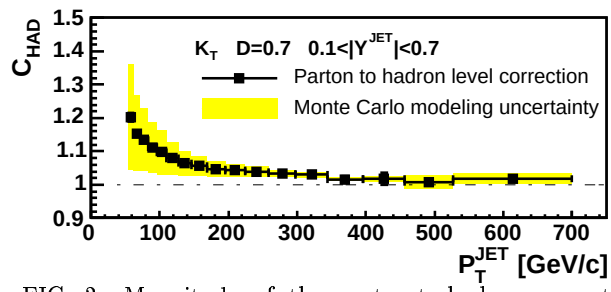

FIG. 2. Magnitude of the parton-to-hadron correction, $C_{HAD}(P_T^{jet})$, used to correct the NLO pQCD predictions. The shaded band indicates the quoted Monte Carlo modeling uncertainty.

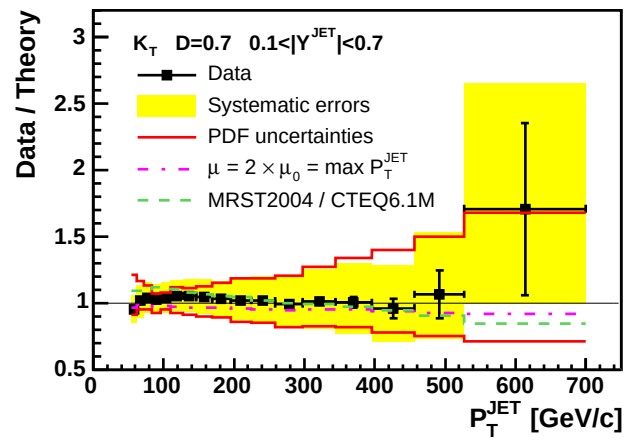

FIG. 3. Ratio Data/Theory as a function of P_T^{jet} for jets with $P_T^{jet} > 54$ GeV/c and $0.1 < |Y^{jet}| < 0.7$. The error bars (shaded band) show the total statistical (systematic) uncertainty on the data. An additional 5.8% uncertainty on the total luminosity is not included in the figure. The solid lines indicate the PDF uncertainty on the theoretical prediction using CTEQ6.1M with $\mu_{R,F}$ set to $\mu_0 = \max(P_T^{jet})/2$. The dashed line presents the ratio of MRST2004 and CTEQ6.1M pQCD predictions. The dotted-dashed line shows the ratio of CTEQ6.1M predictions with $\mu_{R,F}$ set to $2\mu_0$ and μ_0.

In summary, we have presented results on inclusive jet production in $p\overline{p}$ collisions at $\sqrt{s} = 1.96$ TeV using the K_T algorithm with $D = 0.7$, for jets with transverse momentum $P_T^{jet} > 54$ GeV/c and jet rapidity in the region $0.1 < |Y^{jet}| < 0.7$, based on 385 pb^{-1} of CDF Run II data. The measured cross section is in agreement with NLO pQCD predictions. These results confirm the validity of the K_T algorithm to search for jets in a hadron-hadron environment, and will contribute to a better determination of the gluon distribution inside the proton.

Acknowledgments

P_T^{jet} (GeV/c)	$\frac{d^2\sigma}{dP_T^{jet}dY^{jet}} \pm$ (stat.) $\pm$ (sys.) (nb/GeV/c)	$C_{HAD} \pm$ (stat.) $\pm$ (sys.) parton $\rightarrow$ hadron
54 - 62	$(14.6 \pm 0.2^{+1.6}_{-1.6}) \times 10^0$	$1.202 \pm 0.013 \pm 0.158$
62 - 72	$(6.53 \pm 0.04^{+0.75}_{-0.84}) \times 10^0$	$1.154 \pm 0.003 \pm 0.113$
72 - 83	$(2.81 \pm 0.02^{+0.30}_{-0.30}) \times 10^0$	$1.134 \pm 0.005 \pm 0.094$
83 - 96	$(1.179 \pm 0.008^{+0.131}_{-0.125}) \times 10^0$	$1.113 \pm 0.006 \pm 0.077$
96 - 110	$(5.04 \pm 0.04^{+0.56}_{-0.54}) \times 10^{-1}$	$1.098 \pm 0.004 \pm 0.066$
110 - 127	$(2.15 \pm 0.02^{+0.25}_{-0.22}) \times 10^{-1}$	$1.079 \pm 0.005 \pm 0.047$
127 - 146	$(8.81 \pm 0.05^{+1.04}_{-0.98}) \times 10^{-2}$	$1.064 \pm 0.003 \pm 0.037$
146 - 169	$(3.45 \pm 0.02^{+0.46}_{-0.41}) \times 10^{-2}$	$1.057 \pm 0.004 \pm 0.030$
169 - 195	$(1.276 \pm 0.006^{+0.17}_{-0.17}) \times 10^{-2}$	$1.047 \pm 0.003 \pm 0.023$
195 - 224	$(4.67 \pm 0.02^{+0.74}_{-0.68}) \times 10^{-3}$	$1.043 \pm 0.003 \pm 0.018$
224 - 259	$(1.63 \pm 0.01^{+0.30}_{-0.27}) \times 10^{-3}$	$1.039 \pm 0.004 \pm 0.015$
259 - 298	$(5.08 \pm 0.06^{+1.02}_{-0.93}) \times 10^{-4}$	$1.034 \pm 0.003 \pm 0.010$
298 - 344	$(1.50 \pm 0.03^{+0.36}_{-0.31}) \times 10^{-4}$	$1.030 \pm 0.005 \pm 0.008$
344 - 396	$(3.70 \pm 0.14^{+1.07}_{-0.89}) \times 10^{-5}$	$1.016 \pm 0.009 \pm 0.006$
396 - 457	$(7.50 \pm 0.55^{+2.52}_{-2.01}) \times 10^{-6}$	$1.017 \pm 0.018 \pm 0.009$
457 - 527	$(1.31 \pm 0.22^{+0.57}_{-0.42}) \times 10^{-6}$	$1.009 \pm 0.003 \pm 0.019$
527 - 700	$(1.14 \pm 0.43^{+0.63}_{-0.47}) \times 10^{-7}$	$1.018 \pm 0.002 \pm 0.016$

TABLE I. Measured inclusive jet differential cross section as a function of P_T^{jet} for jets with $P_T^{jet} > 54$ GeV/c and $0.1 < |Y^{jet}| < 0.7$ corrected to the hadron level. An additional 5.8% uncertainty on the total luminosity is not included. The parton-to-hadron correction factors, $C_{HAD}(P_T^{jet})$, are applied to the pQCD NLO predictions.

We thank the Fermilab staff and the technical staffs of the participating institutions for their vital contributions. This work was supported by the U.S. Department of Energy and National Science Foundation; the Italian Istituto Nazionale di Fisica Nucleare; the Ministry of Education, Culture, Sports, Science and Technology of Japan; the Natural Sciences and Engineering Research Council of Canada; the National Science Council of the Republic of China; the Swiss National Science Foundation; the A.P. Sloan Foundation; the Bundesministerium fuer Bildung und Forschung, Germany; the Korean Science and Engineering Foundation and the Korean Research Foundation; the Particle Physics and Astronomy Research Council and the Royal Society, UK; the Russian Foundation for Basic Research; the Comision Interministerial de Ciencia y Tecnologia, Spain; in part by the European Community's Human Potential Programme under contract HPRN-CT-2002-00292; and the Academy of Finland.

[1] D.J. Gross and F. Wilczek, Phys. Rev. **D8**, 3633 (1973). H.Fritzsch, M. Gell-Mann and H. Leutwyler, Phys. Lett. **B47**, 365 (1973).
[2] J. Pumplin et al., JHEP **07**, (2002) 012.
[3] A. D. Martin, R.G. Roberts, W. J. Stirling, R. S. Thorne, Eur. Phys. J. C**23**, (2002) 73.
[4] T. Affolder et al., CDF Collab., Phys. Rev. **D64**, 032001 (2001).
B. Abbott et al., *DØ* Collab., Phys. Rev. Lett. **82** 2451 (1999).
[5] The rapidity is defined as $Y = \frac{1}{2}\ln(\frac{E+p_z}{E-p_z})$, where E denotes the energy and p_z is the component of the momentum along the proton beam direction. The pseudorapidity is defined as $\eta = -\ln(\tan(\frac{\theta}{2}))$, where the polar angle θ is taken with respect to the proton beam direction.
[6] S. Catani, Yu.L. Dokshitser, M.H. Seymour and B.R. Webber, Nucl. Phys. **B406** 187 (1993).
[7] S.D. Ellis and D.E. Soper, Phys. Rev. **D48**, 3160 (1993).
[8] The hadronic final state in the Monte Carlo generators is defined using particles with lifetime above 10^{-11}s.
[9] W.T. Giele, E.W.N. Glover and David A. Kosower, Nucl. Phys. **B403**, 633-670 (1993).
[10] D. Acosta et al., CDF Collab., in preparation.
[11] V.M. Abazov et al., *DØ* Collab.,Phys.Lett. **B525** 211 (2002).
[12] D. Acosta et al., CDF Collab., Phys. Rev. D **71** 112002 (2005).
[13] V.M. Abazov et al., *DØ* Collab., submitted to Phys. Rev. Lett. [arXiv:hep-ex/0409040 (2004)].
[14] CDF II Collab., FERMILAB-PUB-96/390-E (1996).
D. Acosta et al., Phys. Rev. D **71**,032001 (2005).
[15] A. Sill et al., Nucl. Instrum. Meth. A **447**, 1 (2000).
A. Affolder et al., Nucl. Instrum. Meth. A **453**, 84 (2000).
C.S. Hill, Nucl. Instrum. Meth. A **530**, 1 (2000).
[16] T. Affolder et al., Nucl. Instr. Meth. A**526**, 249 (2004).
[17] L. Balka et al., Nucl. Instr. Meth. A**267**, 272 (1988).
[18] S. Bertolucci et al., Nucl. Instr. Meth. A **267**, 301 (1988).
[19] R. Oishi, Nucl. Instr. Meth. A **453**, 277 (2000).
[20] D. Acosta et al., Nucl. Instrum. Meth., A **494**, 57 (2002).
[21] R. Brun et al., Technical Report CERN-DD/EE/84-1, CERN, 1987.
[22] G. Grindhammer, M. Rudowicz and S. Peters, Nucl. Instrum. Meth. A 290 (1990) 469.
[23] T. Sjöstrand et al., Comp. Phys. Comm. 135 (2001) 238.
[24] G. Corcella et al., JHEP 0101 (2001) 010.
[25] H.L. Lai *et al.*, Eur. Phys. J. C**12**, 375 (2000)
[26] PYTHIA-Tune A is defined using the tuned parameters in PYTHIA: PARP(67) = 4.0, MSTP(82) = 4, PARP(82) = 2.0, PARP(84) = 0.4, PARP(85) = 0.9, PARP(86) = 0.95, PARP(89) = 1800.0, PARP(90) = 0.25.
[27] D. Acosta et al., CDF Collab., Phys. Rev. D **65**, 092002 (2002).
[28] B. Andersson et al., Phys. Rep. **97**, 31 (1983).
[29] T. Sjöstrand, Comp. Phys. Comm. **39**, 347 (1986).
[30] B.R. Webber, Nucl. Phys. B **238**, 492 (1984).
[31] B. L. Winer, Int. J. Mod. Phys. A **A16S1C**, 1169 (2001).
[32] S.R. Hahn, et al., NIM A **267**, 351 (1988).
[33] P. Bagnaia et al., The UA2 Collab., Phys. Lett. **B144**, 283 (1984).
[34] Olga Norniella, PhD. Thesis, Universitat Autònoma de Barcelona, in preparation.
[35] A. Bhatti et al.,NIM (in preparation).
[36] J. Pumplin et al., CTEQ Collab., Phys. Rev. **D65**, 014013 (2002).